Serb. Astron. J. № 189 (2014), 15 - 24 **UDC 524.726 M31 : 524.354–77**
DOI: 10.2298/SAJ140505002G Original scientific paper

20 cm VLA RADIO-CONTINUUM STUDY OF M 31 – IMAGES AND POINT SOURCE CATALOGUES DR2: EXTRACTION OF A SUPERNOVA REMNANT SAMPLE

T. J. Galvin and M. D. Filipović

University of Western Sydney, Locked Bag 1797, Penrith South DC, NSW 2751, Australia
E–mail: *136525304@student.uws.edu.au, m.filipovic@uws.edu.au*

(Received: May 5, 2014; Accepted: September 2, 2014)

SUMMARY: We present Data Release 2 of the Point Source Catalogue created from a series of previously constructed radio-continuum images of M 31 at λ=20 cm (ν=1.4 GHz) from archived VLA observations. In total, we identify a collection of 916 unique discrete radio sources across the field of M 31. Comparing these detected sources to those listed by Gelfand et al. (2004) at λ=92 cm, the spectral index of 98 sources has been derived. The majority (73%) of these sources exhibit a spectral index of α <–0.6, indicating that their emission is predominantly non-thermal in nature, which is typical for background objects and Supernova Remnants (SNRs). Additionally, we investigate the presence of radio counterparts for some 156 SNRs and SNR candidates, finding a total of only 13 of these objects in our images within a 5″ search area. Auxiliary optical, radio and X-ray catalogues were cross referenced highlighting a small population of SNRs and SNR candidates common to multi frequency domains.

Key words. catalogs – ISM: supernova remnants – radio continuum: galaxies – techniques: image processing

1. INTRODUCTION

As a member of the Andromeda constellation, M 31 is the closest spiral galaxy to our own at a distance of $\sim$ 778 Kpc (Karachentsev et al. 2004). For this reason, it plays a significant role in galactic and extragalactic studies. A number of previous radio-continuum studies at λ=20 cm (Braun 1990a) focused on general properties of M 31, such as its structure and magnetic fields. Also, Braun (1990b) presented a list of 5340 sources in the north-east parts of M 31 at 20 cm. A number of other studies, such as Dickel et al. (1982), estimated flux densities of M 31 supernova remnants (SNRs) and HII regions. Lee et al. (2014) identified 76 new SNRs based on Hα and [SII] images of M 31, and further confirmed a total of 80 SNR candidates from previous literature based on their selection criteria.

In this paper we release our first revision of the data catalogue first published in Galvin et al. (2012). The original catalogue was produced from Very Large Array (VLA) archive data that was accessed and imaged from the National Radio Astronomy Observatory (NRAO) online data retrieval system at λ=20 cm. Here, we also investigate the SNR component of our sample of radio sources in the M 31.

2. DATA AND IMAGE CREATION

A collection of existing, archived radio-continuum observations at λ=20 cm with pointings centred on M 31 were obtained from the National Radio Astronomy Observatory (NRAO)[1] online data retrieval system. In total, 15 VLA projects with a variety of array configurations were selected for use in this study, as summarised in Table 1 of Galvin et al. (2012). These projects were observed between the 1st of October 1983 and 27th of September 1997 and are comprised of 28 individual observational runs.

The MIRIAD (Sault et al. 1995) and KARMA (Gooch 1996) software packages were used for data reduction and analysis. Initially, observations were loaded into AIPS and had their source coordinates converted from the B1950 to the J2000 reference frame. They were then exported to FITS files so that they could be loaded into the MIRIAD software package, which was then used to perform actual data reduction. Typical calibration, flagging and imaging procedures were then carried out (Sault et al. 1995). For more information on data analysis and image creation, as well as the complete set of final images used for source identification, see Galvin et al. (2012), Galvin et al. (2014), O'Brien et al. (2013) and Payne et al. (2004a).

3. RESULTS

Using the images produced in Galvin et al. (2012), we re-evaluate the unique source catalogue produced through that work. Table 1 lists all the sources and the images in which they were found. Using a 2″ search radius, the source catalogue from Galvin et al. (2012) was internally cross referenced to identify sources which were found in more then one image. In such cases, the collection of sources was given an unique group identification number. For each of these groups, an average flux and associated error was calculated based on the individual measurements of each source in that particular group. In total, 916 unique sources were identified, of which 109 were found in at least two images.

In Fig. 1 we present the distribution of flux densities of all unique point sources. For unique sources found in more then one image (a group), that group's average flux was used. Of the total 916 unique sources, 882 (∼96%) are with flux density that is below 50 mJy. From Fig. 1 we estimate that our completeness level is ∼2 mJy.

In Fig. 2 we show the distribution of the average flux errors of each group (109 in total). The majority of source groups (70 out of 109) have errors which are less then 30%. Of the 109 source groups, 17 have an error that is greater then 50%, possibly indicating a population of transient sources in the field of M 31.

Our catalogue was then compared to Gelfand et al. (2004). They identified 405 sources at λ = 92cm though a VLA survey conducted in an A type configuration. Their catalogue also focused predominately on compact radio sources, as the longer baselines of the A type configuration resolved out most of the extended emission. Using a 5″ tolerance, a total of 98 sources were found to be common between both catalogues. We estimate a spectral index ($S_\nu \propto \nu^\alpha$) for these 98 sources using flux density measurements at λ=20 and 92 cm. In the event where a λ=92 cm source was matched to a group of sources from this study (i.e. a source found in more then one image), that group's average flux was used in the derivation of that source's spectral index. The distribution of these spectral indices is presented in Fig. 3. These sources exhibit a predominately negative spectral index, indicating a significant population of background sources and/or SNRs in M 31 field.

4. SNRs IN THE M 31

Magnier et al. (1995) presented a comprehensive study of optically identified SNRs and SNR candidates in the field of M 31. Despite relatively poor seeing conditions (> 2″), short exposure times and imaging only a portion of M 31's complete field, a total of 179 SNRs and SNR candidates were identified. An additional 55 SNRs and SNR candidates were also included in Magnier et al. (1995) from earlier work by Dodorico et al. (1980), Blair et al. (1981) and Braun and Walterbos (1993). These 234 SNRs and SNR candidates were reviewed individually by Lee et al. (2014). Of the 239 SNR candidates presented by Magnier et al. (1995), 154 were discounted by Lee et al. (2014) using their SNR selection criteria.

We compared our radio-continuum catalogue to Lee et al. (2014), who used Hα and [SII] images of M 31 from the Local Group Survey (LGS; Massey et al. 2006) to identify SNR candidates. Using a search criteria of S[II]/Hα > 0.4, morphology and absence of blue stars, they identified a total of 156 SNRs and SNR candidates. Of these 156, some 80 had been listed in previous studies. We searched for these 156 objects in our own catalogue using a 5″ search radius. A total of 13 optical SNR candidates from Lee et al. (2014) were found to have radio counterparts. Some 3 of these 13 were also detected in Gelfand et al. (2004) listed sources. These three sources, J004102+410427, J004339+412653 and J004047+405525, have spectral indices of –0.87, –0.75 and –0.31 respectively. Two SNRs with steeper spectrum are indicative of younger SNR age. Although the relatively steep spectral index of J004102+410427 is more indicative of background galaxy, this source is likely to be intrinsic to M 31 given that it lies on the ring of diffuse emission surrounding the galaxy. We also compared positions from our radio-continuum catalogue presented here and from Lee et al. (2014), and found

[1] https://archive.nrao.edu/archive/e2earchivex.jsp

no significant discrepancy (see Fig. 4). The standard deviations for ΔRA and ΔDec of these 13 sources in common are $1\farcs4$ and $1\farcs3$ respectively, and have been marked in Table 1 with a * (also noted in the table caption).

In Fig. 5 we present a radio-continuum image of M 31 that was produced in Galvin et al. (2012), overlaid with the positions of 156 SNRs and SNR candidates identified by Lee et al. (2014). The red circle represents an SNR that had been previously identified through earlier studies, while the blue cross represents new SNR identified by Lee et al. (2014). We see a large portion of SNRs fall on, or nearby, the ring of emission which surrounds the galaxy. The spatial distribution of these SNR candidates and their coincidence with the ring of diffuse emission implies that there is a higher rate of star formation in the outer arms of the galaxy then in its central region. Sources common between our study and Lee et al. (2014) have been marked with a purple stars.

We also compared our radio-continuum catalogue with Dickel et al. (1982) who observed 10 SNRs in the field of M 31 at λ=20 cm. Of these 10 SNRs, 7 were detected in our VLA images. Once cross-referenced with our own catalogue, we find the 4 strongest detected SNRs listed in Dickel et al. (1982) were present in our own images. These four common sources are J004047+405526, J004513+413616, J004135+410657 and J004513+413616 (Group Identification Number of 92), and note that their fluxes are in good agreement. The other three detected SNRs from Dickel et al. (1982) are below our detection limit.

Using existing optical, radio and X-ray catalogues we investigate the SNR population of M 31. A radio-continuum catalogue (ν=1465 MHz), comprised of 58 SNRs and SNR candidates, was presented by Braun and Walterbos (1993). Of these 58 sources, 24 had a signal to noise ratio above 5σ and were included for use in this study. Comparing our catalogue to the 24 Braun and Walterbos (1993) SNRs, we find that there are 8 matches within a $5''$ search radius. Of the remaining unmatched 16 SNRs some 14 have associated extended emission structure in our images. In Fig. 6 we present a radio-continuum image of M 31 that was produced in Galvin et al. (2012) overlaid with the positions of the 24 Braun and Walterbos (1993) sources with a signal to noise ratio above 5σ. The red circles represent sources common to both, our and Braun and Walterbos (1993) study, while the purple crosses represent sources from Braun and Walterbos (1993) that remained unmatched when compared to our work.

Additionally, 47 X-ray SNRs and SNR candidates were identified by Sasaki et al. (2012) using the *XMM-Newton* telescope. Comparing Sasaki et al. (2012) to our catalogue, we find at total of 11 sources in common.

Fig. 7 is a Venn diagram showing the source intersection of these three catalogues using a search radius of $5''$. It is not surprising that there is only <10% (13 out of 156) coincidences between optical SNRs and SNR candidates and their potential radio counterparts. While in the Magellanic Clouds the ratio between known radio and optical SNRs are $\sim$ 90% (Bozzetto et al. 2014 in prep., Haberl et al. 2012, Filipović et al 2005, 2008, Payne et al. 2004b, 2007, 2008) in other nearby galaxies this ratio is on the order of 10%. For example: NGC 300 ratio is 14% (Millar et al. 2011, 2012), NGC 7793 ratio is 23% (Pannuti et al. 2011, Galvin et al. 2014 in prep.) and NGC 55 ratio is 10% (O'Brien et al. 2013). This may indicate that either our present searches for SNRs in the M 31 are not complete and/or they are biased towards the optical detection implying optical criteria to be bit more sensitive.

At the same time, we point out that the various density environments in which SNRs are expanding also have an effect on their detections. While radio and X-ray observations are biased towards the detections of SNRs embedded in higher density environments, optical searches are more sensitive toward SNRs in low density mediums (see Pannuti et al. 2000). Coupling this with the larger distances to external galaxies (and therefore poorer resolution and sensitivity), our searches for external SNRs are at the moment introducing significant selection effects. Therefore, any comparison of SNRs in external galaxies should be taken with great caution.

5. CONCLUSION

We present version 2 of our point source catalogue of M 31 that was created using archived VLA data at λ=20 cm. In total, 916 unique sources were identified across 15 various VLA projects. Of these 916 sources, 109 were found in at least two different images. The spectral index for 98 sources was derived by comparing our catalogue to Gelfand et al. (2004), who list sources at λ=92 cm. Also, we compared the optical SNR search results of Lee et al. (2014) to our radio-continuum maps of M 31, showing 13 SNRs and SNR candidates in common to two surveys to reside on the ring of diffuse emission surrounding the galaxy. Auxiliary optical, radio and X-ray catalogues were cross referenced highlighting a small population of SNRs and SNR candidates common to multi frequency domains.

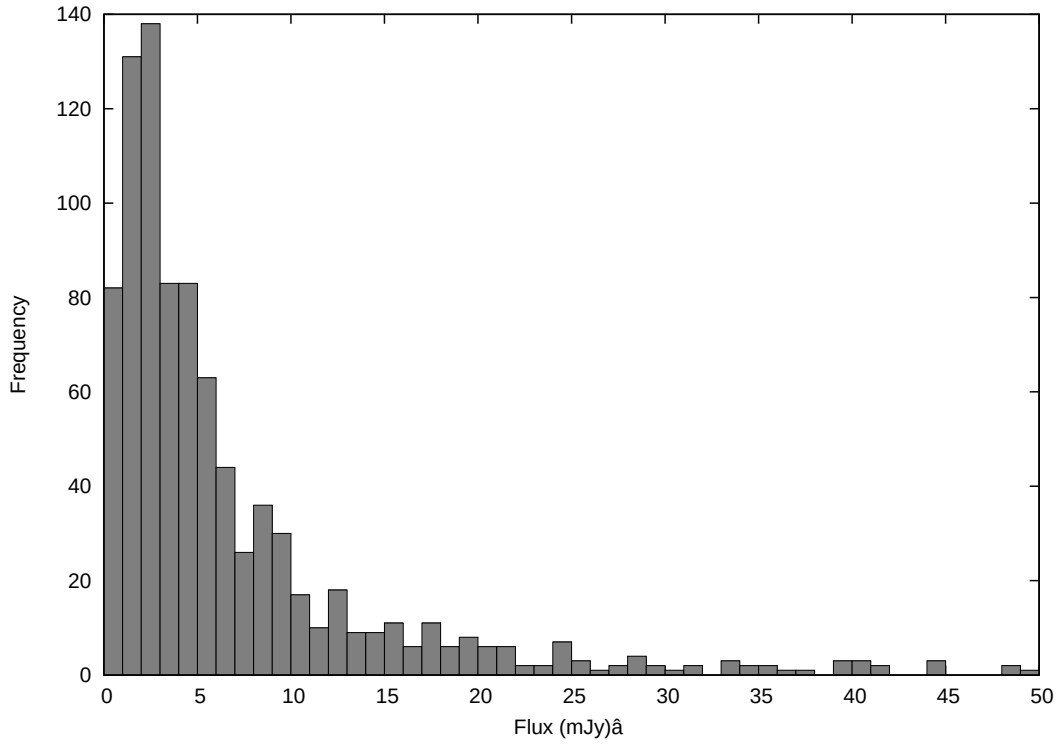

Fig. 1. *The distribution of flux densities for 916 radio sources found in M 31. 34 sources, whose flux density was above 50 mJy, have been excluded from this graph.*

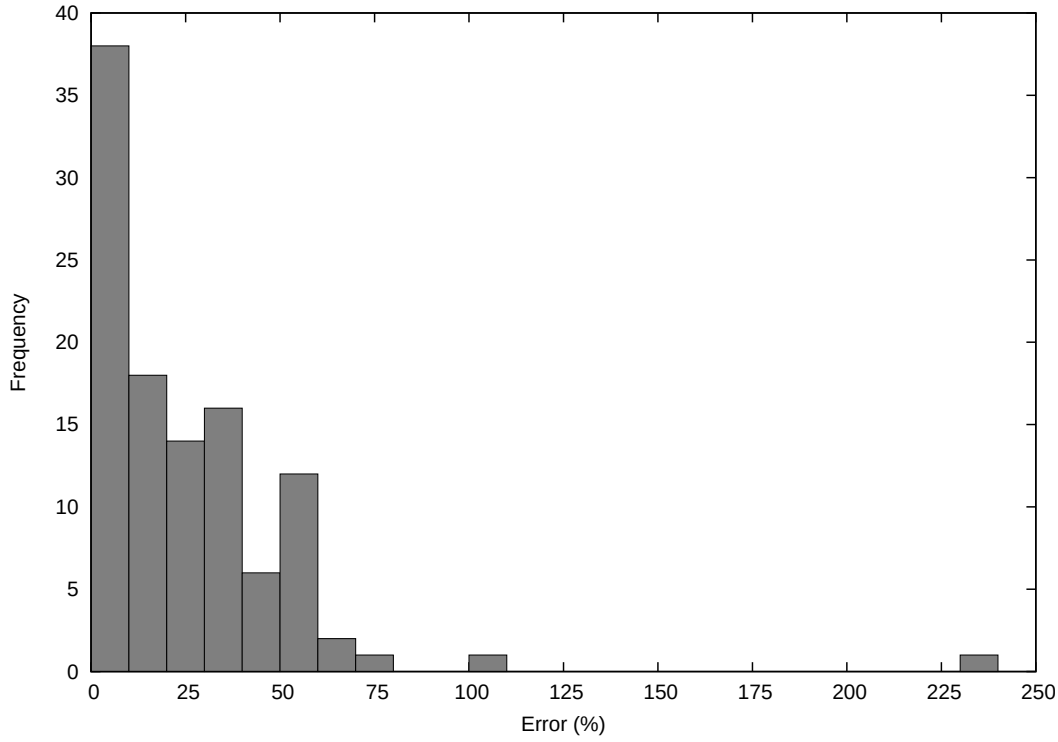

Fig. 2. *The distribution of errors for the average flux density in each group of unique sources.*

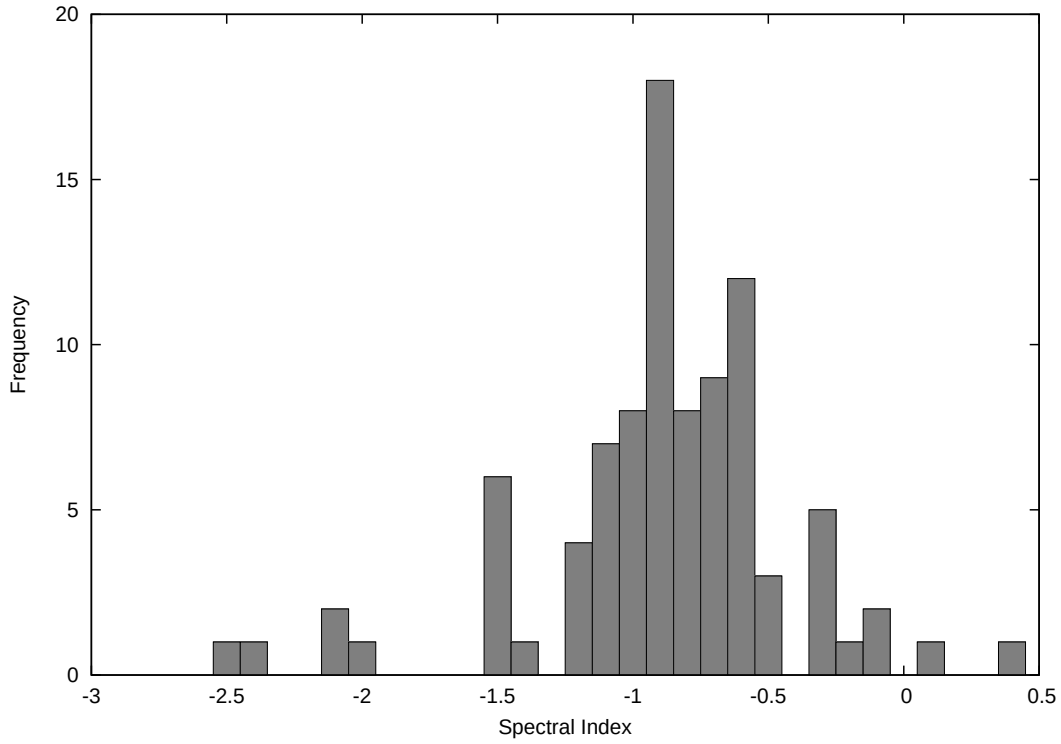

Fig. 3. *Spectral index distribution of 98 point sources in the field of M 31.*

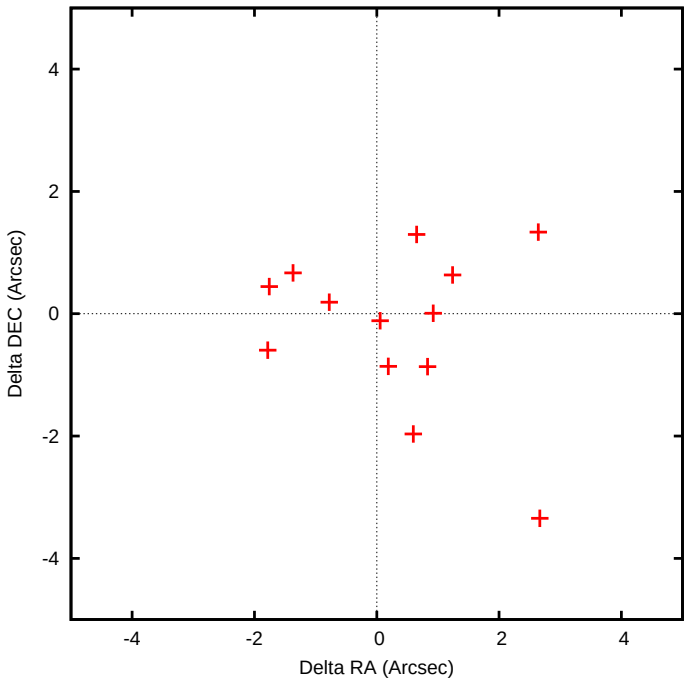

Fig. 4. *RA and Dec offsets of 13 SNRs and SNR candidates common between this study and Lee et al. (2014). The standard deviations for ΔRA and ΔDec are 1.4″ and 1.3″ respectively.*

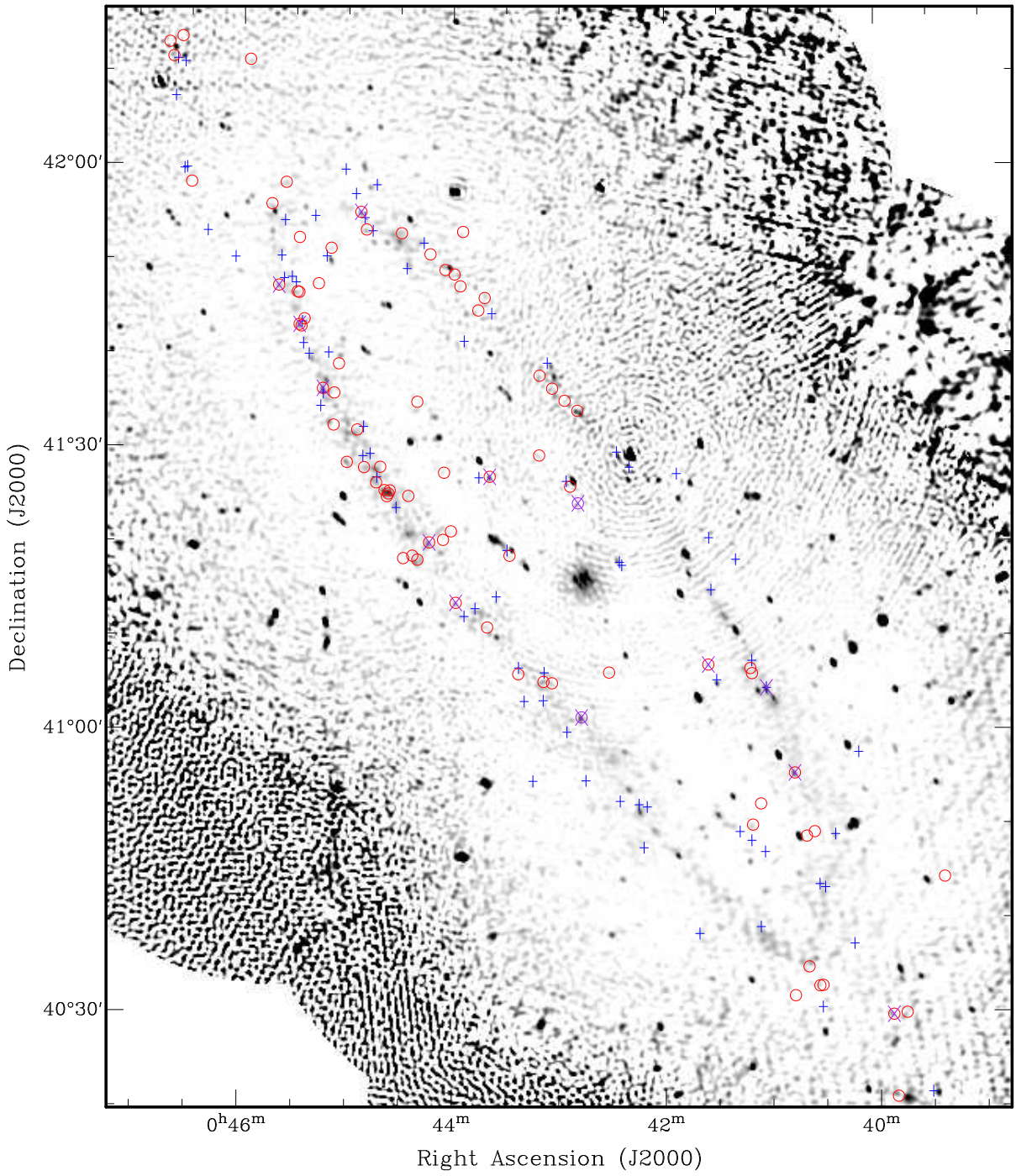

Fig. 5. *A radio-continuum image of M 31 from Galvin et al. (2012) overlaid with the positions of SNRs identified by Lee et al. (2014). The red circles represent all previously identified SNRs that were presented in Lee et al. (2014), while the blue crosses represent new SNR candidates identified by Lee et al. (2014). The purple stars highlight sources common both to our study and to that by Lee et al. (2014).*

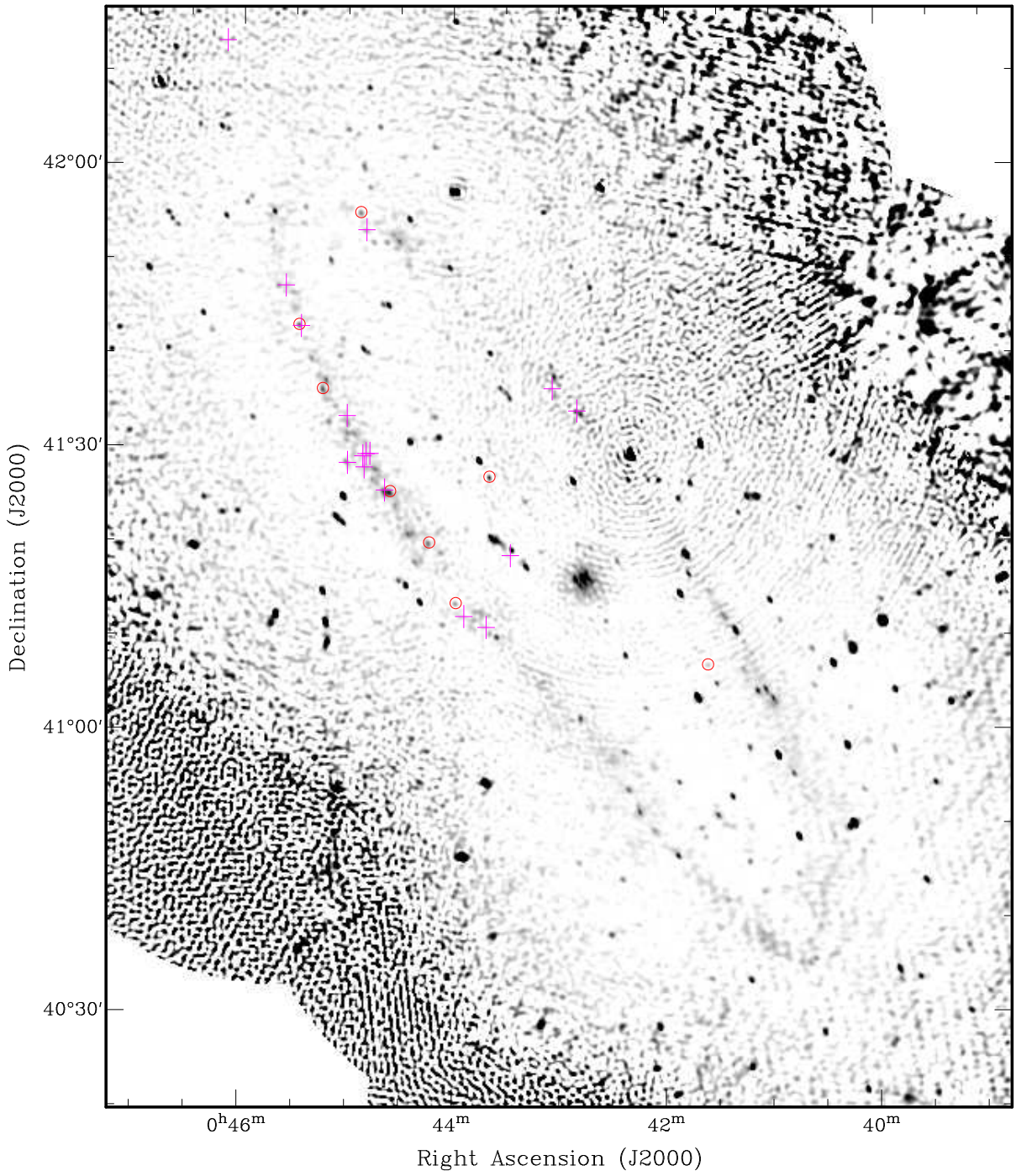

Fig. 6. *A radio-continuum image of M 31 from Galvin et al. (2012) overlaid with the positions of SNRs identified by Braun and Walterbos (1993). The red circles represent sources common to both our study and to the list by Braun and Walterbos (1993), while the purple crosses represent sources in Braun and Walterbos (1993) which did not have a corresponding source in our study.*

Table 1. A summary of all flux density measurements from sources detected in considered projects. Column 1 is the name of the source, Column 2 and Column 3 are the RA and Dec positions (J2000) of each detected source, and Column 4 is the project in which the source was found. Sources common to multiple projects have been assigned a Group ID value, listed in Column 5. The size of each group is listed in Column 6. For each group a mean flux and associated error was calculated and listed in Columns 7 and 8. Columns 9 and 10 are from Gelfand et al. (2004). Column 11 is the spectral index of either Column 4 or Column 8 and Column 10. A source name marked with * indicates that it has an optical counterpart marked as an SNR candidate by Lee et al. (2014).

Name	RA (J2000) h m s	Dec (J2000) ° ′ ″	Flux (mJy)	Project	GroupID	GroupSize	Average (mJy)	Error (%)	GFlux (mJy)	GError Flux (mJy)	Alpha
J003645+404524	00:36:45.82	+40:45:24.40	7.08	AC0308-3							
J003651+404452	00:36:51.36	+40:44:52.40	4.81	AC0308-3							
J003724+403821	00:37:24.96	+40:38:21.30	2.61	AC0308-3							
J003730+401239	00:37:30.21	+40:12:39.10	4.95	AC0308-3							
J003745+402513	00:37:45.61	+40:25:13.50	22.56	AC0308-3							
J003807+405252	00:38:07.88	+40:52:52.90	3.04	AC0308-3					11.16	0.67	-0.85
J003813+403100	00:38:13.13	+40:31:00.80	5.89	AC0308-3							
J003814+403425	00:38:14.44	+40:34:25.70	6.53	AC0308-3							
J003817+405110	00:38:17.55	+40:51:10.90	2.85	AC0308-3							
J003817+410220	00:38:17.91	+41:02:20.30	5.18	AC0308-3							
J003818+410040	00:38:18.16	+41:00:40.30	5.01	AC0308-3							
J003819+405414	00:38:19.60	+40:54:14.40	12.46	AC0308-3							
J003821+404136	00:38:21.04	+40:41:36.70	4.59	AB0437-b							
J003821+411916	00:38:21.55	+41:19:16.20	5.13	AC0308-3							
J003825+413704	00:38:25.63	+41:37:04.10	83.66	AC0308-3							
J003832+413433	00:38:32.35	+41:34:33.60	2.19	AC0308-3							
J003833+404956	00:38:33.37	+40:49:56.20	3.98	AC0308-3							
J003838+415149	00:38:38.95	+41:51:49.20	4.54	AC0308-3							
J003839+403300	00:38:39.00	+40:33:00.60	4.85	AB0437-b							
J003839+412611	00:38:39.00	+41:26:11.10	3.66	AC0308-3							
J003845+403326	00:38:45.20	+40:33:26.50	5.44	AC0308-3							
J003848+395206	00:38:48.51	+39:52:06.60	6.19	AC0308-3							
J003848+411606	00:38:48.75	+41:16:06.40	84.03	AB0437-a							
J003849+411608	00:38:49.05	+41:16:08.60	20.45	AC0308-3							
J003849+411606	00:38:49.59	+41:16:06.81	73.55	AH0524-a							
J003849+411601	00:38:49.66	+41:16:01.30	6.19	AM0464-a							
J003854+401636	00:38:54.51	+40:16:36.60	4.17	AC0308-3							
J003856+403210	00:38:56.74	+40:32:10.60	5.54	AC0308-3							
J003903+403051	00:39:03.17	+40:30:51.50	3.54	AC0308-3							
J003904+410822	00:39:04.30	+41:08:22.20	2.46	AB0437-a							
J003907+410346	00:39:07.94	+41:03:46.10	20.65	AB0437-a							
J003908+403007	00:39:08.25	+40:30:07.71	2.88	AB0437-b							
J003908+410338	00:39:08.28	+41:03:38.21	7.59	AB0437-a							
J003908+410335	00:39:08.39	+41:03:35.80	6.62	AB0437-b							
J003908+403009	00:39:08.78	+40:30:09.99	1.84	AM0464-a							
J003909+403010	00:39:09.25	+40:30:10.40	7.88	AC0308-3							
J003916+403629	00:39:16.37	+40:36:29.37	0.59	AM0464-a							
J003916+410440	00:39:16.51	+41:04:40.90	5.07	AC0308-3							
J003917+410258	00:39:17.98	+41:02:58.90	9.85	AB0437-b							
J003918+405513	00:39:18.13	+40:55:13.90	3.26	AC0308-3							
J003918+410301	00:39:18.15	+41:03:01.10	12.43	AB0437-a							
J003918+410257	00:39:18.16	+41:02:57.30	9.52	AC0308-3							
J003918+411636	00:39:18.45	+41:16:36.30	4.08	AC0308-3							
J003918+411634	00:39:18.88	+41:16:34.06	5.65	AB0437-a							
J003919+402206	00:39:19.50	+40:22:06.08	0.74	AM0464-a							
J003921+411404	00:39:21.24	+41:14:04.90	4.40	AC0308-3							
J003922+411040	00:39:22.15	+41:10:40.95	3.70	AH0524-a							
J003922+411038	00:39:22.16	+41:10:38.50	3.01	AM0464-a							
J003922+411040	00:39:22.43	+41:10:40.10	11.38	AB0437-a							
J003922+411500	00:39:22.87	+41:15:00.80	4.48	AC0308-3							
J003923+411045	00:39:23.05	+41:10:45.50	2.65	AC0308-3							
J003927+405429	00:39:27.28	+40:54:29.00	4.37	AB0437-a							
J003927+405423	00:39:27.43	+40:54:23.60	6.71	AC0308-3							
J003927+402123	00:39:27.61	+40:21:23.46	0.75	AM0464-a							
J003929+414607	00:39:29.72	+41:46:07.60	24.62	AC0308-3							
J003929+415456	00:39:29.75	+41:54:56.30	2.58	AC0308-3							
J003930+410440	00:39:30.87	+41:04:40.10	6.91	AB0437-a							
J003931+411502	00:39:31.09	+41:15:02.08	2.18	AB0437-a							
J003931+411511	00:39:31.41	+41:15:11.85	2.36	AH0524-a							
J003932+410440	00:39:32.22	+41:04:40.71	1.17	AH0524-a							
J003932+404402	00:39:32.71	+40:44:02.30	12.54	AC0308-3							
J003932+400837	00:39:32.83	+40:08:37.90	50.17	AC0308-3					156.98	11.37	-0.75
J003932+404403	00:39:32.95	+40:44:03.50	9.87	AB0437-b							
J003933+404401	00:39:33.02	+40:44:01.40	7.11	AM0464-a							
J003933+404406	00:39:33.06	+40:44:06.40	8.14	AB0437-a							
J003933+400848	00:39:33.12	+40:08:48.00	6.73	AM0464-a							
J003933+404405	00:39:33.35	+40:44:05.34	4.16	AH0221-a							
J003935+411430	00:39:35.87	+41:14:30.69	3.84	AB0437-a							
J003936+411426	00:39:36.29	+41:14:26.10	4.78	AC0308-1							

The complete table is available online at *http://saj.math.rs/189/pdf/Table1.pdf.*

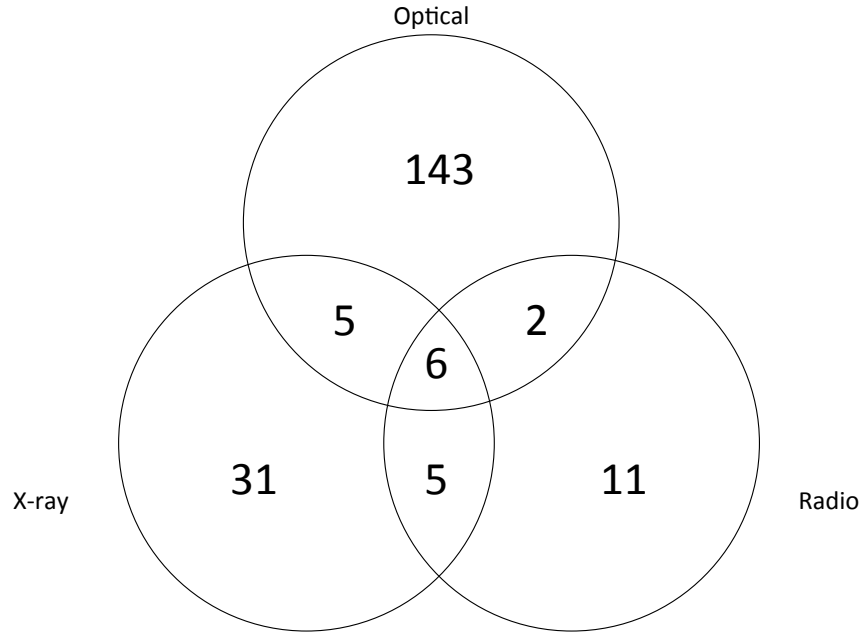

Fig. 7. *Venn Diagram showing the intersection of sources from optical (Lee at al. 2014), radio (Braun and Walterbos 1993) and X-ray (Sasaki et al. 2012) catalogues from SNRs and SNR candidate sources in the field of M 31.*

Acknowledgements – We used the KARMA and MIRIAD software packages developed by the ATNF. The National Radio Astronomy Observatory is a facility of the National Science Foundation operated under cooperative agreement by Associated Universities, Inc.

REFERENCES

Blair, W. P., Kirshner, R. P. and Chevalier, R. A.: 1981, *Astrophys. J.*, **247**, 879.
Braun, R.: 1990a, *Astrophys. J. Suppl. Series*, **72**, 755.
Braun, R.: 1990b, *Astrophys. J. Suppl. Series*, **72**, 761.
Braun, R. and Walterbos, R.: 1993, *Astron. Astrophys. Suppl. Series*, **98**, 327.
Dickel, J. R., Dodorico, S., Felli, M. and Dopita, M.: 1982, *Aust. J. of Phys.*, **252**, 582.
Dodorico, S., Dopita, M. A. and Benvenuti, P.: 1980, *Astron. Astrophys. Suppl. Series*, **40**, 67.
Filipović, M. D., Payne, J. L., Reid, W., Danforth, C. W., Staveley-Smith, L., Jones, P. A. and White, G. L.: 2005, *Mon. Not. R. Astron. Soc.*, **364**, 217.
Filipović, M. D., Haberl, F., Winkler, P. F., Pietsch, W., Payne, J. L., Crawford, E. J., de Horta, A. Y., Stootman, F. H. and Reaser, B. E.: 2008, *Astron. Astrophys.*, **485**, 63.
Galvin, T. J., Filipović, M. D., Crawford, E. J., Tothill, N. F. H., Wong, G. F. and De Horta, A. Y.: 2012, *Serb. Astron. J.*, **184**, 41.
Galvin, T. J., Filipović, M. D., Tothill, N. F. H., Crawford, E. J., O'Brien, A. N., Seymour, N., Pannuti, T. G., Kosakowski, A, R. and Sharma, B.: 2014, *Astrophys. Space Sci.*, **353**, 603.
Gelfand, J. D., Lazio, T. J. W. and Gaensler, B. M.: 2004, *Astrophys. J. Suppl. Series*, **155**, 89.
Gooch, R.: 1996, in "Astronomical Society of the Pacific Conference Series, Vol. 101, Astronomical Data Analysis Software and Systems V", G. H. Jacoby and J. Barnes, ed., 80.
Haberl, F., Sturm, R., Ballet, J., Bomans, D. J., Buckley, D. A. H., Coe, M. J., Corbet, R., Ehle, M., Filipovic, M. D., Gilfanov, M., Hatzidimitriou, D., La Palombara, N., Mereghetti, S., Pietsch, W., Snowden, S. and Tiengo, A.: 2012, *Astron. Astrophys.*, **545**, A128.
Karachentsev, I. D., Karachentseva, V. E., Huchtmeier, W. K. and Makarov, D. I.: 2004, *Astron. J.*, **127**, 2031.
Lee, J. H. and Lee, M. G.: 2014, *Astron. J.*, **786**, 130.
Magnier, E. A., Prins, S., van Paradijs, J., Lewin, W. H. G., Supper, R., Hasinger, G., Pietsch, W. and Truemper, J.: 1995, *Astron. Astrophys. Suppl. Series*, **114**, 215.
Massey, P., Olsen, K. A. G., Hodge, P. W., Strong, S. B., Jacoby, G. H., Schlingman, W. and Smith, R. C.: 2006, *Astron. J.*, **131**, 2478.
Millar, W. C., White, G. L., Filipović, M. D., Payne, J. L., Crawford, E. J., Pannuti, T. G. and Staggs, W. D.: 2011, *Astrophys. Space Sci.*, **332**, 221.

Millar, W. C., White, G. L. and Filipović, M. D.: 2012, *Serb. Astron. J.*, **184**, 19.
O'Brien, A. N., Filipović, M. D., Crawford, E. J., Tothill, N. F. H., Collier, J. D., De Horta, A. Y., Wong, G. F., Drašković, D., Payne, J. L., Pannuti, T. G., Napier, J. P., Griffith, S. A., Staggs, W. D. and Kotuš, S.: 2013, *Astrophys. Space Sci.*, **347**, 159.
Pannuti, T. G., Duric, N., Lacey, C. K., Goss, W. M., Hoopes, C. G., Walterbos, R. A. M. and Magnor, M. A.: 2000, *Astrophys. J.*, **544**, 780.
Pannuti, T. G., Schlegel, E. M., Filipović, M. D., Payne, J. L., Petre, R., Harrus, I. M., Staggs, W. D. and Lacey, C. K.: 2011, *Astron. J.*, **142**, 20.
Payne, J. L., Filipović, M. D., Pannuti, T. G., Jones, P. A., Duric N., White, G. L. and Carpano, S.: 2004a, *Astron. Astrophys.*, **425**, 443.
Payne, J. L., Filipović, M. D., Reid, W., Jones, P. A., Staveley-Smith, L. and White, G. L.: 2004, *Mon. Not. R. Astron. Soc.*, **355**, 44.
Payne, J. L., White, G. L., Filipović, M. D. and Pannuti, T. G.: 2007, *Mon. Not. R. Astron. Soc.*, **376**, 1793.
Payne, J. L., White, G. L. and Filipović, M. D.: 2008, *Mon. Not. R. Astron. Soc.*, **383**, 1175.
Sasaki, M., Pietsch, W., Haberl, F., Hatzidimitriou, D., Stiele, H., Williams, B., Kong, A. and Kolb, U.: 2012, *Astron. Astrophys.*, **544**, A144.
Sault, R. J., Teuben, P. J. and Wright, M. C. H.: 1995, in "Astronomical Society of the Pacific Conference Series, Vol. 77, Astronomical Data Analysis Software and Systems IV", R. A. Shaw, H. E. Payne and J. J. E. Hayes, ed., 433.

АНАЛИЗА VLA ПОСМАТРАЊА ГАЛАКСИЈЕ M 31 НА 20 cm У РАДИО-КОНТИНУУМУ – СЛИКЕ И КАТАЛОГ ТАЧКАСТИХ ИЗВОРА DR2: ИЗДВАЈАЊЕ УЗОРКА ОСТАТАКА СУПЕРНОВИХ

T. J. Galvin and M. D. Filipović

University of Western Sydney, Locked Bag 1797, Penrith South DC, NSW 1797, Australia
E–mail: *136525304@student.uws.edu.au, m.filipovic@uws.edu.au*

УДК 524.726 M31 : 524.354–77
Оригинални научни рад

Представљамо верзију 2 нашег каталога тачкастих радио-извора у галаксији M 31 на λ=20 cm (ν=1.4 GHz). Укупно смо идентификовали 916 дискретних радио-објеката позиционираних у пољу M 31. Упоређивањем нашег каталога са каталогом Gelfand et al. (2004) на λ=92 cm, нашли смо 98 заједничких објеката за које смо израчунали спектралне индексе. Већина (73%) ових објеката има спектралне индексе $\alpha < -0.6$, из чега следи да је нетермална емисија доминантна — типично за позадинске галаксије и остатке супернових. Такође, истраживали смо и постојање радио-детекција за 156 познатих остатака супернових детектованих оптичким посматрањима и нашли смо 13 таквих објеката. Упоређивања са додатним оптичким, радио и X каталозима указују на малу популацију остатака супернових који се могу детектовати на свим овим фреквенцијама.